

AD-A037350

WVT-TR-77001

TECHNICAL
LIBRARY

COMPUTER CONTROLLED X-RAY STRESS ANALYSIS
FOR INSPECTION OF MANUFACTURED COMPONENTS

G.P. CAPSIMALIS
R.F. HAGGERTY
K. LOOMIS

January 1977



BENET WEAPONS LABORATORY
WATERVLIET ARSENAL
WATERVLIET, N.Y. 12189

TECHNICAL REPORT

AMCMS No. 3297.06.7282

Pron No. M1-4-A1527

APPROVED FOR PUBLIC RELEASE; DISTRIBUTION UNLIMITED

DISCLAIMER

The findings in this report are not to be construed as an official Department of the Army position unless so designated by other authorized documents.

The use of trade name(s) and/or manufacturer(s) in this report does not constitute an official indorsement or approval.

DISPOSITION

Destroy this report when it is no longer needed. Do not return it to the originator.

4

20.
problem solutions using FORTRAN IV,

All operations of the stress goniometer, the modular electronic hardware, logic operations and data processing are performed in real time and are completely computer controlled.

TABLE OF CONTENTS

INTRODUCTION	1
THEORETICAL BACKGROUND	2
EXPERIMENTAL APPROACH	6
A. INSTRUMENTATION	6
B. SOFTWARE	9
C. PROCEDURE FOR ALIGNMENT OF THE SIEMENS STRESS GONIOMETER	10
EXPERIMENTAL RESULTS	12
A. X-RAY ELASTIC CONSTANT	12
B. STRESS DISTRIBUTION IN AUTOFRETTAGED TUBES	13
DISCUSSION	13
REFERENCES	27

LIST OF FIGURES

FIGURE 1 ILLUSTRATION OF STRESS STRAIN ANGULAR RELATIONS USED IN X-RAY MEASUREMENT	15
FIGURE 2 BLOCK DIAGRAM OF THE AUTOMATED X-RAY STRESS SYSTEM	16
FIGURE 3 FLOWCHART FOR THE STRESCAN PROGRAM	17
FIGURE 4 INPUT FORMAT FOR STRESCAN	18
FIGURE 5 OUTPUT FORMAT FROM STRESCAN	19
FIGURE 6 TTY OUTPUT OF STRESS VS. $\sin^2\psi$	20
FIGURE 7 X-RAY MEASURED STRESS VS. APPLIED STRESS FOR THE CALIBRATION TEST BAR	21

FIGURE 8	THE RADIAL DISTRIBUTION OF HOOP STRESS IN A 155MM AUTOFRETTAGED GUN TUBE	22
FIGURE 9	THE RADIAL DISTRIBUTION OF HOOP STRESS FOR AN AUTOFRETTAGED 175MM TUBE WITH 30% OVERSTRAIN	23
FIGURE 10	SCHEMATIC DIAGRAM OF THE STRESS GONIOMETER	24
FIGURE 11	VIEW OF STRESS GONIOMETER AND GUN TUBE SECTION BEING INSPECTED	25
FIGURE 12	CLOSE UP VIEW OF COMPUTER AND AUTOMATION ELECTRONICS HARDWARE	26

INTRODUCTION

Residual stresses are present in gun tubes either inadvertently due to heat treatment forging, cold strengthening, or deliberately due to autofrettage. The effects of residual stresses on the mechanical and physical behavior of gun steel and other structural materials are well established; they can drastically alter the fatigue properties of the structure and cause warping and corrosion cracking.

Undesirable stresses may result from either variations in steels or machining practices and can remain undetected prior to the observation of their adverse effects. The objective of this effort was to develop an automated x-ray stress system to provide support to engineering development, manufacturing, and quality control. Automation was required to permit acquisition of quality data which otherwise would be very laborious and tedious to obtain by manual means. Finally this system should accommodate on-line data analysis including correction for instrumental and physical factors, least squares curve fitting and essentially instant printout of the results.

This report describes the automated x-ray stress system developed which minimizes the possibility of human error and significantly reduces the time and cost of the stress analysis.

THEORETICAL BACKGROUND¹⁻³

The principle of x-ray stress analysis is based upon the measurement of lattice strains of specially oriented sets of lattice planes which are then related to stress by means of the elasticity relations which will be shown in this section.

For a homogeneous isotropic elastic solid, strain ϵ is defined by the relation

$$\epsilon = \frac{\Delta l}{l} \quad (1)$$

where Δl is the change in length of a stressed solid having an original length l .

If we take a rectangular coordinate system and a strain ϵ_x produced by a stress σ_x alone acting in the x-direction, then Hooke's law requires that:

$$\epsilon_x = \frac{\sigma_x}{E} \quad (2)$$

where E is Young's modulus.

If a tensile stress is applied in the x-direction it will produce a linear elongation in the x-direction and a linear contraction in the transverse y and z-directions. The longitudinal and transverse strains are related by:

$$-\epsilon_y = -\epsilon_z = \nu \epsilon_x = \frac{\nu \sigma_x}{E}, \quad (3)$$

where ν is Poisson's ratio, and ϵ_y and ϵ_z the transverse strains in the y and z-directions.

¹C. S. Barrett and T. B. Massalski, "Structure of Metals", New York: McGraw Hill, 1966.

²E. Macherauch, "X-Ray Stress Analysis", Proc. Soc. Exp. Mechanics, 23, 140 (1966).

³J 784, "Residual Stress Measurements by X-Ray Diffraction", New York: Autom. Engr. (1971).

For a triaxial system with the coordinate axes along the principal stress directions, the principal stresses are related to the principal strains as follows:

$$\epsilon_1 = \frac{1}{E} [\sigma_1 - \nu(\sigma_2 + \sigma_3)] \quad , \quad (4a)$$

$$\epsilon_2 = \frac{1}{E} [\sigma_2 - \nu(\sigma_1 + \sigma_3)] \quad , \quad (4b)$$

$$\epsilon_3 = \frac{1}{E} [\sigma_3 - \nu(\sigma_1 + \sigma_2)] \quad , \quad (4c)$$

At a free surface, the normal stress is zero, i.e., $\sigma_3 = 0$.

Therefore:

$$\epsilon_1 = \frac{1}{E} (\sigma_1 - \nu\sigma_2) \quad , \quad (5a)$$

$$\epsilon_2 = \frac{1}{E} (\sigma_2 - \nu\sigma_1) \quad , \quad (5b)$$

$$\epsilon_3 = \frac{1}{E} (\sigma_1 + \nu\sigma_2) \quad . \quad (5c)$$

From Figure 1 the stress $\sigma_{\phi\psi}$ is given by

$$\sigma_{\phi\psi} = \sigma_1 (\sin\psi \cos\phi)^2 + \sigma_2 (\sin\psi \sin\phi)^2 \quad , \quad (6)$$

Similarly the normal strain $\epsilon_{\phi\psi}$ is given by:

$$\epsilon_{\phi\psi} = \epsilon_1 (\sin\psi \cos\phi)^2 + \epsilon_2 (\sin\psi \sin\phi)^2 + \epsilon_3 \cos^2\psi \quad , \quad (7)$$

from equations (5) and (7) we obtain

$$\epsilon_{\phi\psi} = \frac{1+\nu}{E} (\sigma_1 \cos^2\phi + \sigma_2 \sin^2\phi) \sin^2\psi - \frac{\nu}{E} (\sigma_1 + \sigma_2) \quad (8)$$

But the surface stress component σ_ϕ is given by:

$$\sigma_\phi = \sigma_1 \cos^2\phi + \sigma_2 \sin^2\phi \quad , \quad (9)$$

Therefore, substituting in Eq. 8

$$\epsilon_{\phi\psi} = \left(\frac{1+\nu}{E}\right) \sigma_\phi \sin^2\psi - \frac{\nu}{E} (\sigma_1 + \sigma_2) \quad . \quad (10)$$

From equation 5c we have:

$$\epsilon_3 = -\frac{\nu}{E} (\sigma_1 + \sigma_2) \quad (11)$$

Substituting in equation (10) and rearranging we obtain:

$$\sigma_\phi = (\epsilon_{\phi\psi} - \epsilon_3) \frac{E}{1+\nu} \frac{1}{\sin^2\psi} \quad (12)$$

Let d be the interplanar spacing normal to the plane surface, and d_0 its value in the stress free state and d_ψ in the direction specified by the angle ψ , then

$$\epsilon_{\phi\psi} - \epsilon_3 = \frac{d_\psi - d_0}{d_0} \frac{d - d_0}{d_0}$$

$$\epsilon_{\phi\psi} - \epsilon_3 = \frac{d_\psi - d_0}{d_0}$$

or

$$\epsilon_{\phi\psi} - \epsilon_3 \approx \frac{d_\psi - d}{d} \quad (13)$$

Substituting equation (13) in (12) gives

$$\sigma_\phi = \frac{d_\psi - d}{d} \frac{E}{1+\nu} \frac{1}{\sin^2\psi} \quad (14)$$

Differentiating the Bragg law

$$n\lambda = 2d\sin\theta \quad (15)$$

we obtain

$$\frac{\Delta d}{d} = -\cot\theta\Delta\theta \quad (16)$$

Combining (16) and (14) we obtain

$$\sigma_\phi = -\Delta\theta \cot\theta \left(\frac{E}{1+\nu}\right) \frac{1}{\sin^2\psi}$$

which is equivalent to

$$\sigma_\phi = (2\theta - 2\theta_\psi) \frac{\cot\theta}{2} \left(\frac{E}{1+\nu}\right) \frac{1}{\sin^2\psi} \quad (17)$$

Equations (10) and (17) provide the fundamental relations for x-ray stress measurements.

An examination of equation (10) shows that

- a. The lattice strains $\epsilon_{\phi\psi}$ are linearly dependent on $\sin^2\psi$.
- b. If the lattice strains $\epsilon_{\phi\psi}$ for several ψ angles are measured and plotted vs. $\sin^2\psi$, the slope, m , of the line is:

$$m = \frac{\partial \epsilon_{\phi\psi}}{\partial (\sin^2\psi)} = \frac{\nu+1}{E} \sigma_{\phi} \quad , \quad (18)$$

$$\text{or } \sigma_{\phi} = \frac{E}{\nu+1} m. \quad (19)$$

It can readily be seen that very accurate stress measurements can be obtained even with some scatter in the x-ray data when a least squares fit is used to obtain the slope of the line (strain vs. $\sin^2\psi$). A second advantage of this method is that, unlike other residual stress measuring techniques, it is not necessary to obtain a reference measurement from a completely unstressed sample. Finally, anomalous stresses can be generated under certain conditions of uniaxial plastic deformation⁴. These are manifested by a non-linear behavior of the σ_{ϕ} vs. $\sin^2\psi$ curve. The above technique permits detection of these anomalous contributions and will help identify the non-linearity which characterizes pseudo stresses.

⁴B. D. Cullity, "Sources of Error in X-Ray Measurements of Residual Stress", J. Appl. Phys. 35, No. 6, 1915 (1964).

EXPERIMENTAL APPROACH

There are two general ways of measuring residual stresses by means of x-ray diffraction namely: the photographic and the diffractometric method. The principal reason for selecting the diffractometer over the photographic method is that it provides a very precise and objective means of locating the diffraction peaks. This is especially desirable when dealing with the broad diffraction profiles commonly found in hardened steels. The diffractometric procedure is also capable of complete automation thus permitting major improvements in the techniques which otherwise would be prohibitively laborious and time consuming.

A. INSTRUMENTATION

The hardware of the computer controlled system described below are shown in the form of a block diagram in Figure 2.

STRESS GONIOMETER⁸

The automated x-ray unit is a Siemens-goniometer powered by a Phillips x-ray generator.

³J 784, "Residual Stress Measurements by X-Ray Diffraction", New York: Autom. Engr. (1971).

⁵D. P. Koistiuen, and R. E. Marburger, "Calculating Peak Position in X-Ray Residual Stress Measurements of Hardened Steel", Trans. Am. Soc. Metals, 51, 537 (1959).

⁶C. J. Kelly and E. Eichen, "Computer Controlled X-Ray Diffraction Measurement of Residual Stress" in L. S. Birks, C. S. Barrett, J. B. Newkirk and C. O. Rudd, Editors, Advances in X-Ray Analysis, 16, 344, Plenum Press (1973).

⁷G. Koves and C. Y. Ho, "Computer Automated X-Ray Stress Analysis", Norelco Reporter, 11, 99 (1964).

⁸N. W. Tideswell, I. Canner, and H. J. Vanderveldt, "Field X-Ray Diffractometer for Surface Stress Determinations in Naval Structures", Naval Ship Research and Development Center, Report 3568, April 1972.

The Siemens stress goniometer was selected for several reasons. The unit is portable and has been designed to measure stresses on large test items. Determinations of peak positions of diffraction profiles are made with precision comparable to that of laboratory diffractometers because the unit can be made to satisfy the stationary Bragg-Bretano geometry where the detector remains on the diffractometer circle. Currently the automated unit allows stress determination to be made either from the two or multi exposure $\sin^2\psi$ method. The two exposure $\sin^2\psi$ procedure allows a more precise stress measurement to be performed. This is accomplished by averaging out the random scatter of the intensity data points and thus each point contributes significantly towards higher accuracy of the stress measurement.

The modification made for automation of the goniometer was the replacement of the 2θ continuous motor drive and the manual ψ drive with two remotely controllable Slo-Syn stepping motors. The motors were attached to the 2θ and ψ drive shafts using specially machined adaptors. The automation of the goniometer functions and data gathering is accomplished by means of the Canberra computer oriented electronics shown in Figure 2 and described below.

TELECOMPUTER

The telecomputer interface is an executive module which provides full duplex serial communication between the system modules and the minicomputer or teletype. The interface executes a set of ten programmable commands which direct the positioning, counting and recording functions of the other system-compatible modular instruments.

DUAL COUNTER/TIMER

This module is a programmable two channel counting device capable of either preset count or preset time operation. In the manual mode the functions of the counter/timer are controlled manually from the front panel. In the remote operation mode each channel responds to its own coded two digit address to perform commands which are received from the telecomputer interface.

DUAL AXIS POSITIONERS

These modular units are devices for driving the stepping motors which control the 2θ and ψ axes of the goniometer. Each axis positioner responds to its own individual address and by means of the telecomputer interface is controlled remotely from instructions generated from the minicomputer.

THE MINICOMPUTER

A Digital Equipment PDP11/05 minicomputer provides complete control of the system functions during data acquisition, performs extensive mathematical operations in processing the data and instantly provides the results in a comprehensive digital and/or graphical manner. The computer configuration shown in Figure 2 consists of a processor with 12K core memory, a large volume 1.2 million word storage disk, a magnetic tape unit and an ASR33 teletype. This configuration supports a Fortran IV computational language which is familiar to most engineers and scientists.

B. SOFTWARE

In addition to the regular DEC supplied software (Fortran IV compiler, utility programs, etc.) an interface program in machine language was developed to allow the user to communicate with the Telecomputer Interface.

RESIDUAL STRESS PROGRAM

Using a program called 'STRESCAN' which was written in FORTRAN IV and implemented on the PDP11/05 minicomputer, the operator can obtain residual measurements under total computer control. A simplified flow chart of the STRESCAN program is shown in Figure 3. A brief description of the program follows.

When the program is referenced, a routine conversation mode develops whereby the operator defines the initial coordinates of the 2θ and ψ axes. The computer further requests the start and stop positions of the scan along with the required step sizes and the initial number of counts to be taken.

The computer then controls the two axes and instructs the motors to drive to the first position. After a quick scan (at the first ψ angle) through the 2θ angular range, a peak is calculated by fitting the corrected intensities to a parabola. This general location of the peak enables a more careful scan with a smaller step size (automatically calculated) and a greater number of counts. The intensity data is then fitted to a parabola with the number of points determined by the operator. The number of counts specified are normally determined by the peak to background ratio obtained from a separate scan. The

calculated peak is then saved for later reference. After the 2θ peak is determined, the ψ angle is incremented by the preset step size.

The above procedure is then repeated until the last ψ angle is reached.

The program then calculates the strains corresponding to the different ψ angles. Finally, the program calculates the stress from a least square fit of ϵ_ψ vs. $\sin^2\psi$. The program printout on the teletype includes 2θ peaks at various ψ settings, the starting 2θ values, adjusted 2θ step sizes, the strains for each ψ , the constant used, the slope calculated, the y-intercept and a plot of the least squares fit of ϵ_ψ vs. $\sin^2\psi$ and finally the stress σ . Figures 4 and 5 show typical STRESCAN input and output formats as they are produced on the teletype.

C. PROCEDURE FOR ALIGNMENT OF SEIMENS STRESS GONIOMETER

The method used to align the Siemens stress goniometer will be described. It consists of three steps: 1) mechanical, 2) optical and 3) 0-stress on gold.

Mechanical alignment is accomplished by adjusting the center of the ϕ semi-circle, along which the x-ray tube and detector travel, and the center of the ψ circle, about which the goniometer rotates, until the two centers coincide with each other and with the axis of a fixed adjusting goniometer column. Figure 10 shows a schematic diagram of the stress goniometer.

Optical alignment consists of adjusting the x-ray beam until the center of the beam and the center of the ϕ and ψ circles coincide at the axis of the fixed adjusting column. The goniometer is now rotated around the ϕ semi-circle and a $1/2^\circ$ beam is observed on a florescent screen (a fine line drawn on the screen aids in this observation). When the beam is aligned, no beam shift should be observed as the ψ axis rotates from 0 to 60 degrees. If a shift occurs an Allen screw located on the side of the entrance aperature system is used to shift the beam at right angles to the beam direction, and the process is repeated. Finer slits can be used for more careful adjustment. With a $1/2^\circ$ entrance aperture slit located in the x-ray entrance system and a 1° aperture slit in front of the detector the goniometer is ready for the final adjustment. A stress-free gold specimen which has been deposited on a glass plate is placed in the specimen holder. The position of the gold line (the gold (222) reflection is at 153° when a chrome tube is used) is determined for $\psi = 0, 10, 20, 30, 40$ and 50 degrees. If the specimen surface is located precisely in the axis, gold lines will be independent of ψ and no stress will be observed since no change in 2θ has occurred.

After the goniometer has been aligned, the distance from the x-ray tube reference plate to the specimen's surface is carefully measured to $1/100$ of a mm. The goniometer can now be rotated away from the reference column, and as long as the measured distance is kept constant, the work piece, surface and the ϕ and ψ centers will coincide.

EXPERIMENTAL RESULTS

During the course of this investigation the automated system has been used to establish standards and procedures for the accurate and reproducible determination of stresses in gun steel. In this section the need for the determination of the x-ray elastic constant will be demonstrated. Also typical stress distribution of autofrettaged gun tubes will be discussed.

A. X-RAY ELASTIC CONSTANT

The basic expressions (12) and (17) used in obtaining the x-ray stress σ_{ϕ} contain the familiar mechanical constants E and ν . Because of the selective way the x-ray method measures strain the use of the mechanical constants E and ν in expression (17) often results in a measured value which deviates from the true stress. This is especially true for materials which are elastically anisotropic.

In the present case a calibration run was made on a flat rectangular test bar of gun steel. The test bar was electropolished on one side to remove machining stresses and a strain gage was mounted on the other side. A four point bending fixture was used to apply successively known amounts of stress (monitored by the strain gage) to the surface of the test bar. The corresponding x-ray stress values were obtained from the measured x-ray strains using expression (12) and the mechanical constants E and ν . A comparison of the measured x-ray stress to the applied stress, shown in Figure 7, reveals that a linear relationship and a small deviation exists between the two stresses. The true x-ray elastic constants can be calculated from eq (18)

$$m = \frac{\nu + 1}{E} \sigma_{\phi}$$

following the procedure of Macherauch.²

B. STRESS DISTRIBUTION IN AUTOFRETTAGE TUBES

Autofrettage is a process that imparts a favorable residual stress distribution to gun tubes and is responsible for greatly extending their service lives.⁹ The automated system was used to determine the radial hoop stress distribution for a 155MM gun tube with 100% overstrain. The x-ray stress results are shown in Figure 8 where a theoretically expected distribution is included for the sake of comparison. Similar results obtained from an autofrettaged 175MM gun tube with 30 overstrain is shown in Figure 9.

DISCUSSION

As already discussed¹⁰ the existence of residual stresses may be beneficial as well as detrimental. The autofrettage process provides a way of extending the elastic pressure range of gun tubes. It also imparts a compressive hoop stress to the bore which effectively limits crack propagation and thus early fatigue failure. The problem of primary importance is to insure that the necessary hoop stress levels are present in autofrettaged tubes. The automated x-ray unit with its

²E. Macherauch, "X-Ray Stress Analysis", Proc. Soc. Exp. Mechanics, 23, 140 (1966).

⁹T. E. Davidson, J. E. Throop, A. N. Reiner, "The Role of Fracture Toughness and Residual Stresses in the Fatigue and Fracture Behavior of Large Thick-Walled Pressure Vessels", Watervliet Arsenal Report No. 7184, October 1971.

¹⁰P. J. Cote and G. P. Capsimalis, "Applications of X-Ray Stress Measuring Techniques", Watervliet Arsenal Report No. 7253, October 1972.

associated computer organization and logic allowed the development of what was considered strictly a manual laboratory technique into an accurate and practical testing method. At the present time it can routinely measure non-destructively the surface stresses of gun tubes and other manufactured components. Additionally this new system for measuring residual stresses is not limited to any specific material such as gun steel, but can be applied to most other metals or alloys employed in defense materials. The system can effectively detect variations in stress levels caused by future changes in manufacturing processes. These technological changes are often required in order to keep pace with demands of new materials, new techniques and improvements in manufacturing methods.

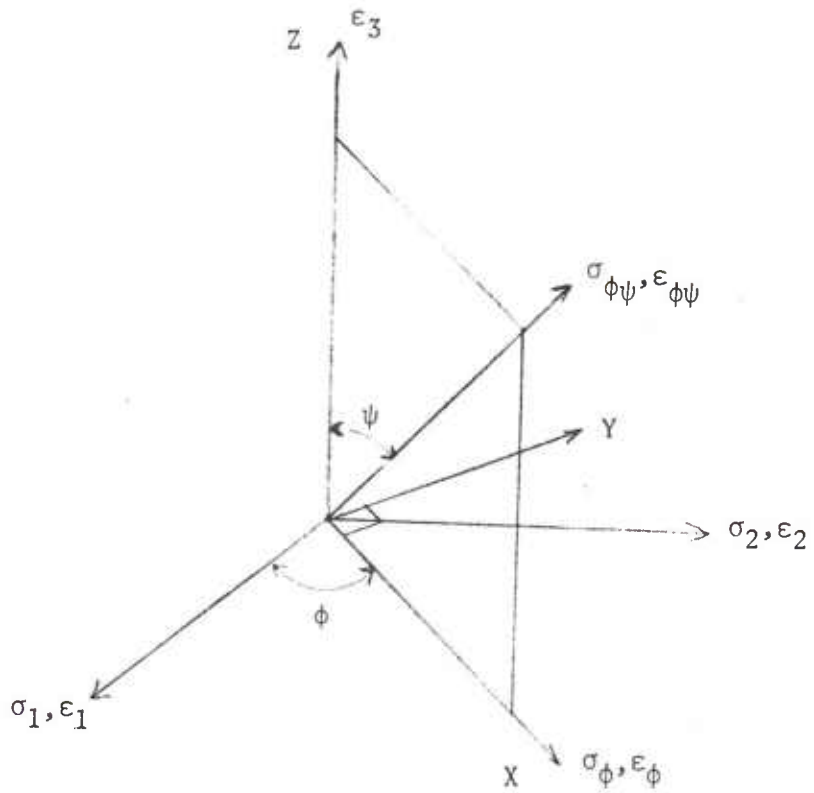


FIG. 1 ILLUSTRATION OF STRESS AND STRAIN ANGULAR RELATIONS USED IN X-RAY MEASUREMENTS.

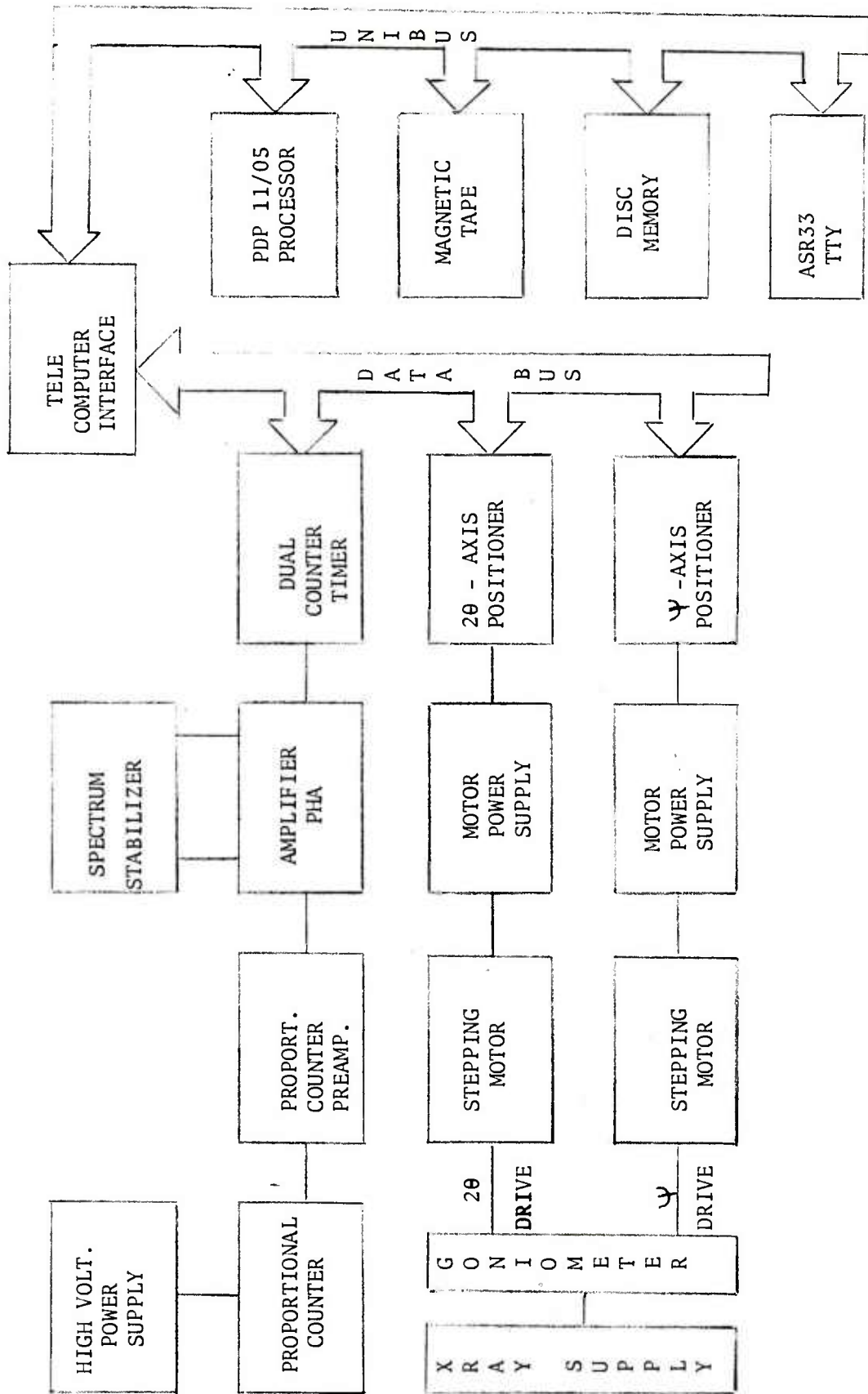


FIG. 2 BLOCK DIAGRAM OF THE AUTOMATED X-RAY STRESS SYSTEM

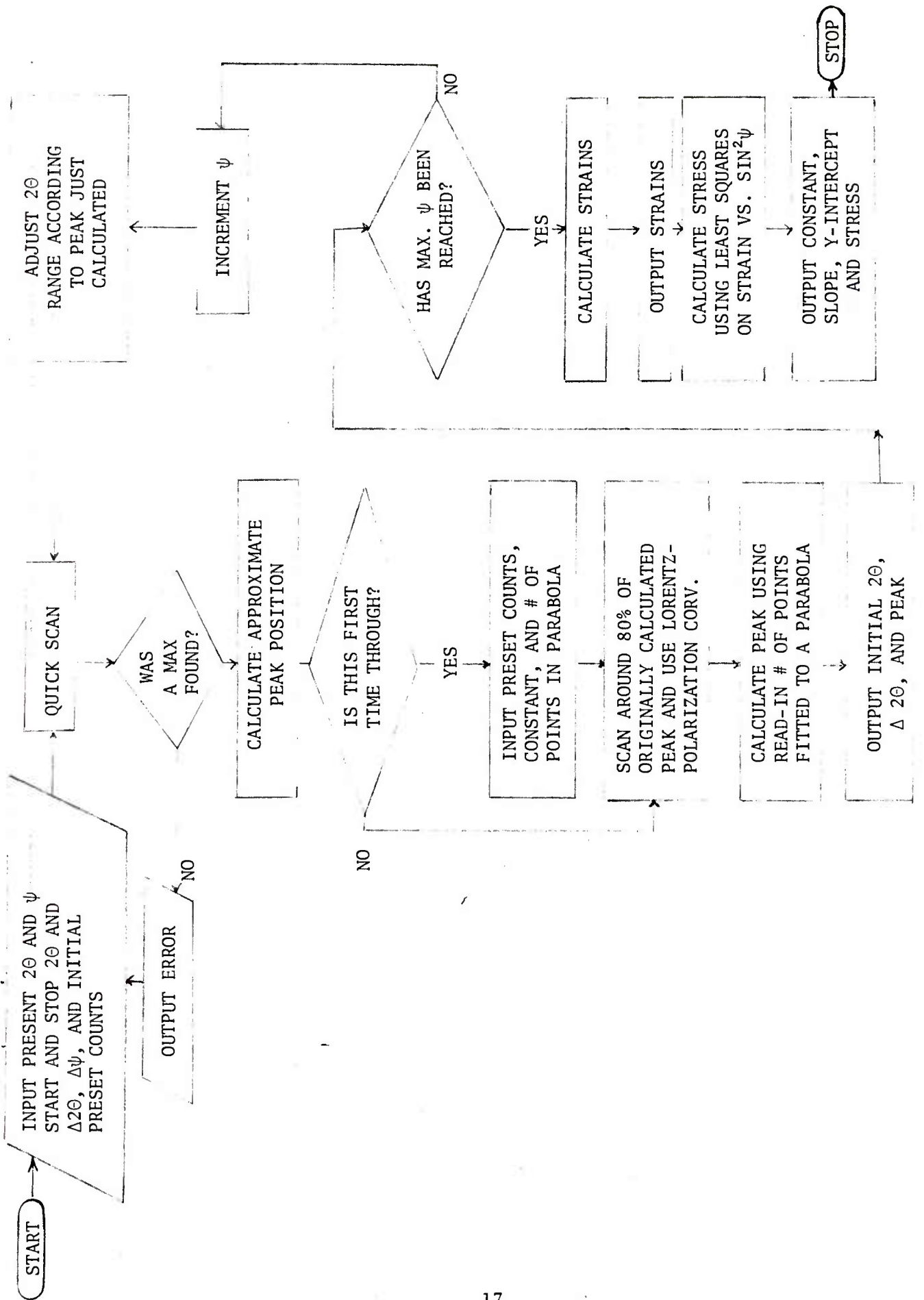


FIG. 3 FLOWCHART FOR THE STRESSCAN PROGRAM

INPUT DIALOGUE FOR A SAMPLE RUN

RU STRESCAN

12-MAR-76

ENTER 2-THETA AND PSI POSITIONS

156.26, 0

ENTER START 2-THETA AND PSI POSITIONS

155.00, 0

ENTER STOP 2-THETA AND PSI POSITIONS

157.00, .50

ENTER 2-THETA AND PSI STEP SIZES

.40, .10

ENTER PRESET COUNTS...INITIAL

23

INITIAL QUICK SCAN OUTPUT:

INTENSITY	2-THETA
-----------	---------

102.209	155.00
---------	--------

174.779	155.40
---------	--------

282.860	155.80
---------	--------

217.157	156.20
---------	--------

185.888	156.00
---------	--------

148.728	157.00
---------	--------

ENTER # OF COUNTS, STRESS CONSP, # OF PTS, FOR PARABOLA

24,2.283E7,5

FIG. 4 SHOWS A TYPICAL INPUT FORMAT OF THE DIALOGUE FROM
A ROUTINE X-RAY STRESS MEASUREMENT

OUTPUT SUMMARY: FOR A SAMPLE RUN

START 2-THETA	2-THETA STEP	2-THETA MAX.
155.45	20.00	155.890
155.45	20.00	155.879
155.45	20.00	155.863
155.43	20.00	155.839
155.42	20.00	155.815
155.40	20.00	155.786

CALCULATED STRAINS

STRAIN	PSI ANGLE
0.21629E-04	0.10000E 02
0.52585E-04	0.20000E 02
0.97273E-04	0.30000E 02
0.14350E-03	0.40000E 02
0.19910E-03	0.50000E 02

RESULTS

SLOPE	Y-INTER.	STRESS
0.31520E-03	0.14742E-04	0.71960E 04

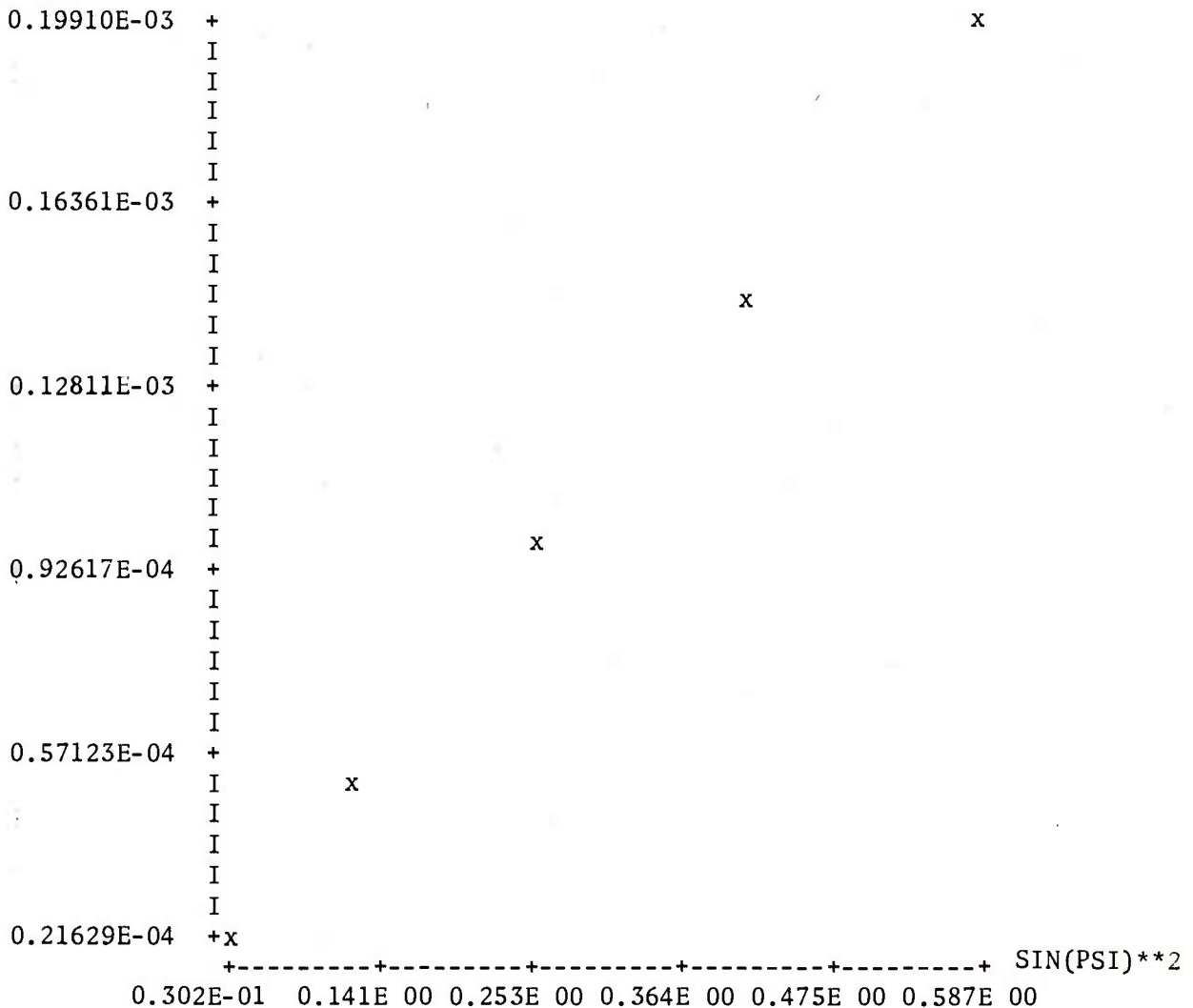
FIG. 5 OUTPUT FORMAT FROM STRESCAN

* RU PLOT

AFTER THE * DEFINE THE DATA SET TO BE PLOTTED
* STRESS·DAT

LINE NO.	SIN (PSI) ** 2	STRAIN
1	0.301540E-01	0.216290E-04
2	0.116980E-00	0.525850E-04
3	0.250000E 00	0.972730E-04
4	0.413180E 00	0.143500E-03
5	0.586820E 00	0.199100E-03

STRAIN



Y-INTERCEPT = 0.147411E-04 SLOPE = 0.315204E-03

FIG. 6 TTY OUTPUT OF STRAIN VS. $\text{SIN}^2\psi$

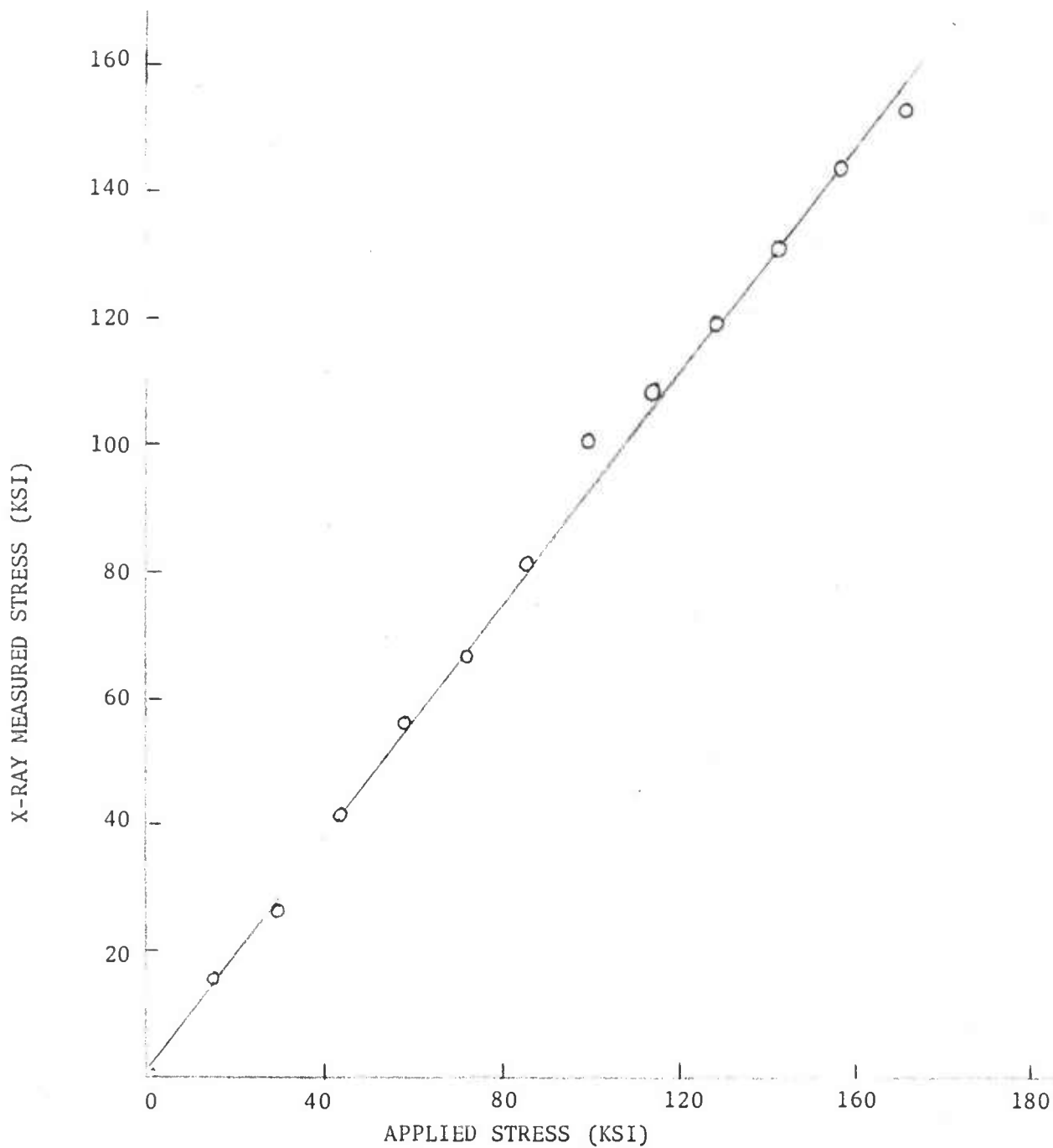


FIG. 7 X-RAY MEASURED STRESS VS. APPLIED STRESS FOR THE CALIBRATION TEST BAR

SOLID CURVE: THEORETICAL EXPECTED DISTRIBUTION
 VERTICAL BAR: X-RAY STRESS VALVE

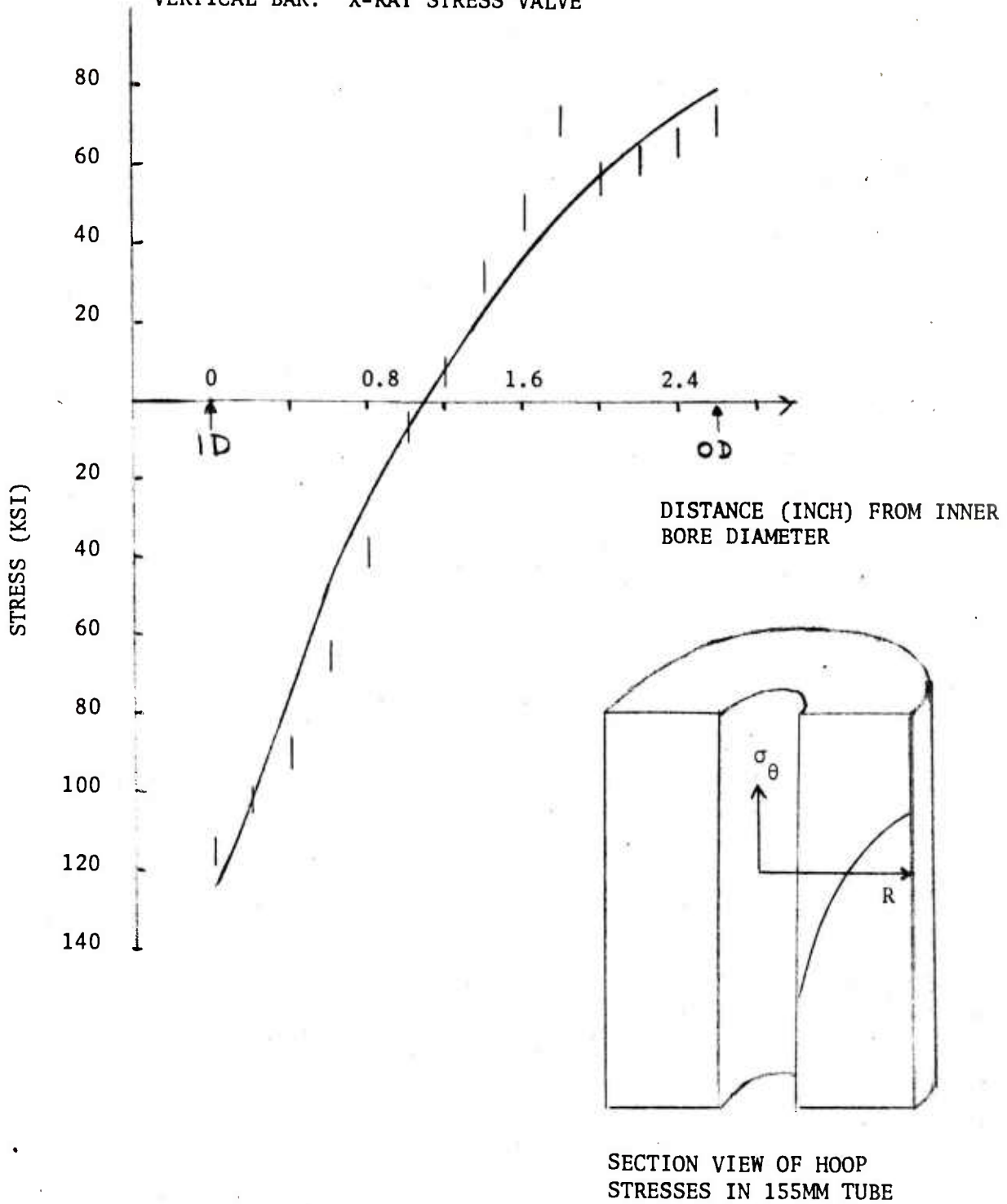
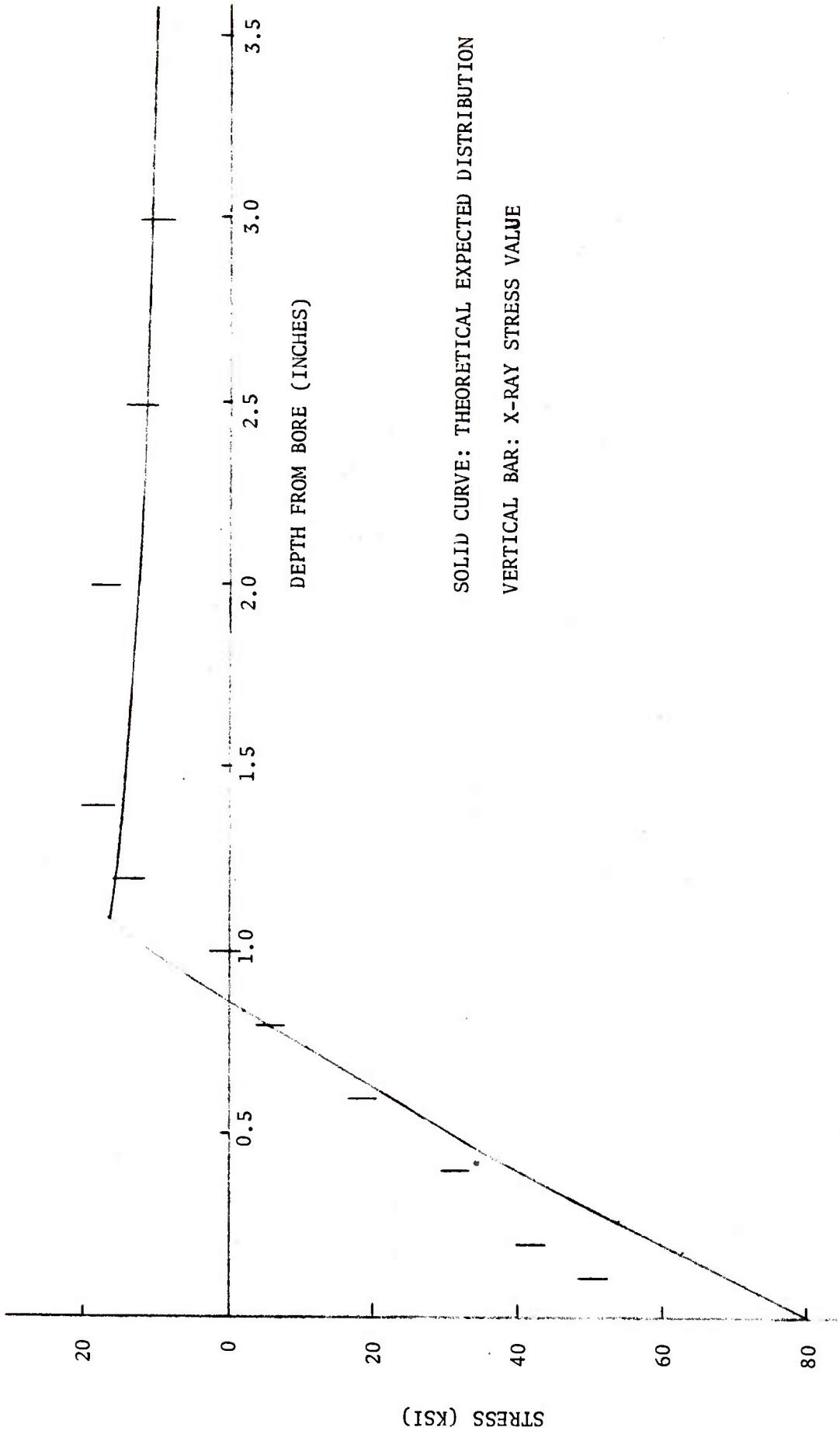


FIG. 8 THE RADIAL DISTRIBUTION OF HOOP STRESS IN A 155MM AUTOFRETTAGE GUN TUBE .



STRESS (KSI)

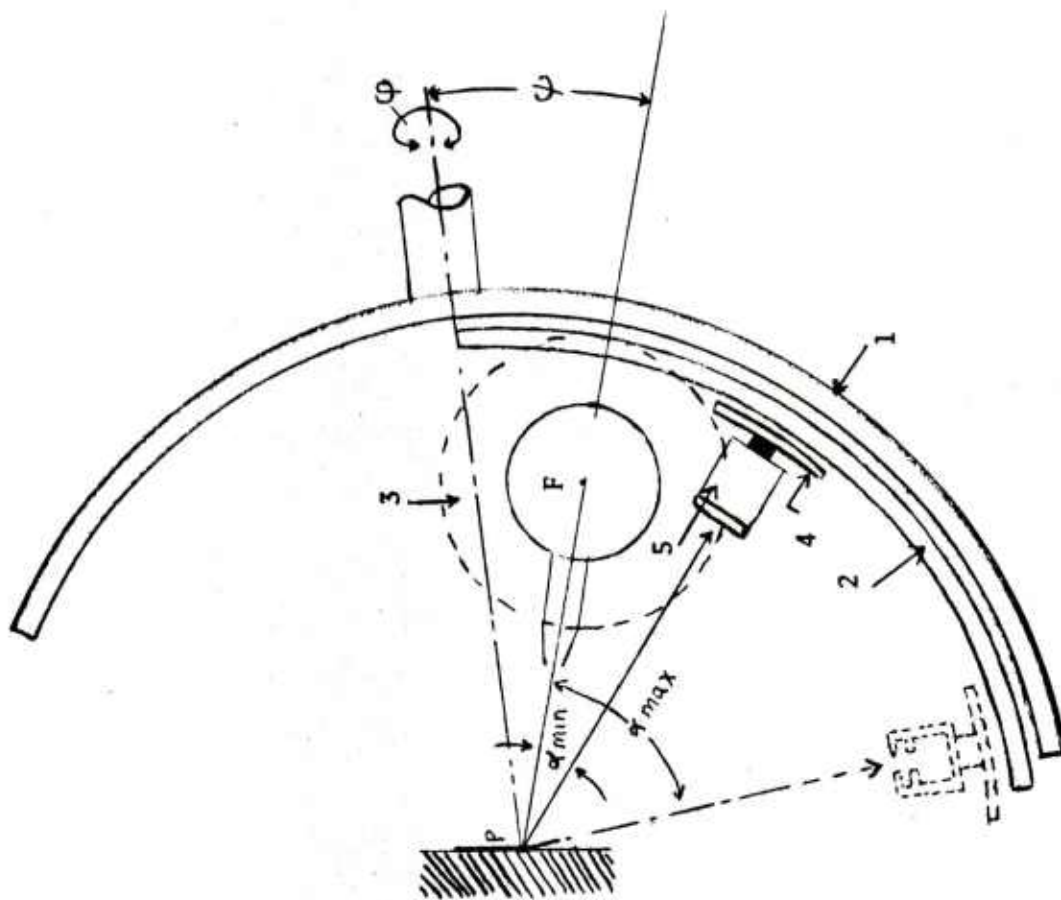
DEPTH FROM BORE (INCHES)

SOLID CURVE: THEORETICAL EXPECTED DISTRIBUTION

VERTICAL BAR: X-RAY STRESS VALUE

FIG. 9 THE RADIAL DISTRIBUTION OF HOOP STRESS FOR AN AUTOFRETTAGED 175MM TUBE WITH 30% OVERSTRAIN

*PROVIDED BY J. F. THROOP, MATERIALS ENGINEERING DIVISION



- 1 SEMI-CIRCULAR RAIL
- 2 SLIDING CARRIAGE
- 3 X-RAY TUBE WITH FOCUS F
- 4 DETECTOR SLIDING CARRIAGE
- 5 DETECTOR

FIG. 10 SCHEMATIC DIAGRAM OF THE STRESS GONIOMETER

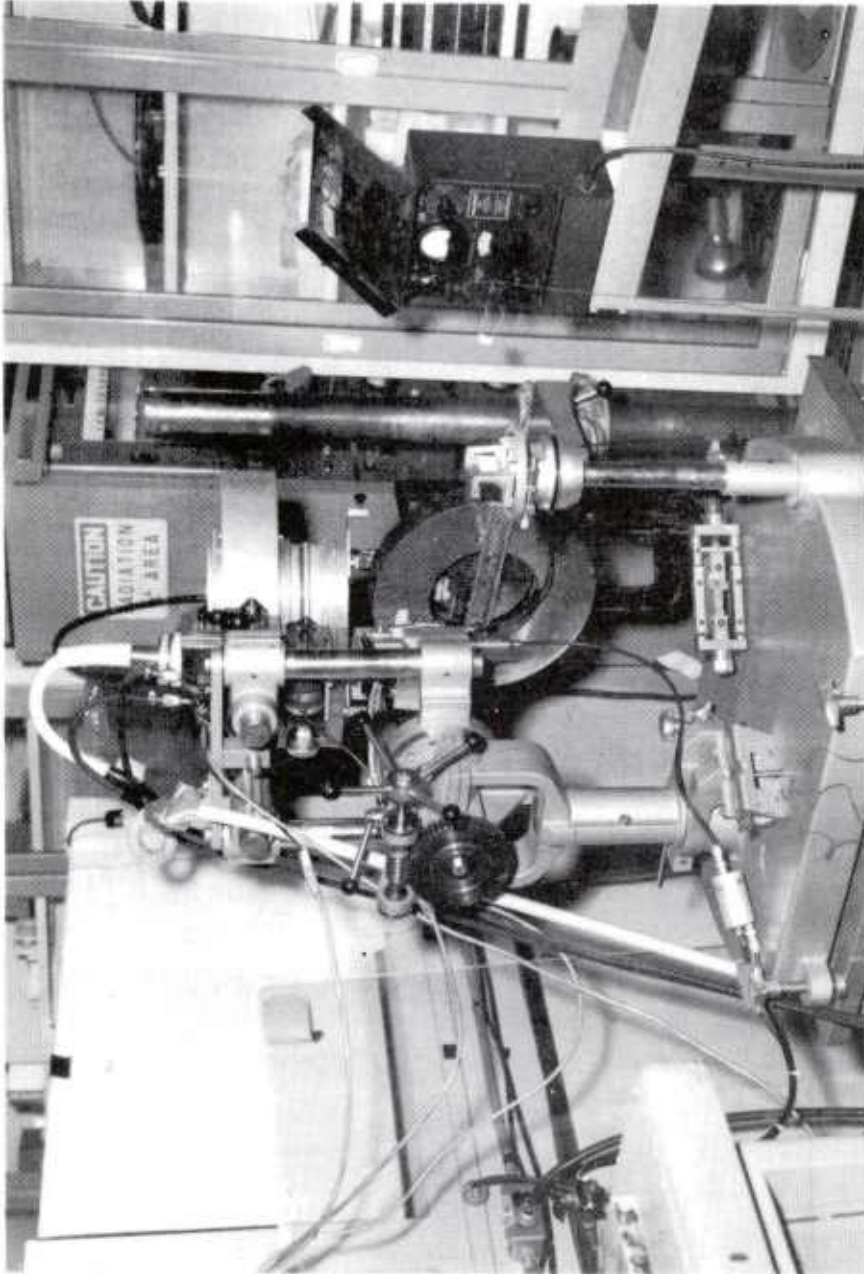


FIG. 11 VIEW OF STRESS GONIOMETER AND GUN TUBE SECTION BEING INSPECTED



FIG. 12 CLOSE UP VIEW OF COMPUTER AND AUTOMATION ELECTRONICS HARDWARE

REFERENCES

1. C. S. Barrett and T. B. Massalski, "Structure of Metals", New York: McGraw Hill, 1966.
2. E. Macherauch, "X-Ray Stress Analysis", Proc. Soc. Exp. Mechanics, 23, 140 (1966).
3. J 784, "Residual Stress Measurements by X-Ray Diffraction", New York: Autom. Engr. (1971).
4. B. D. Cullity, "Sources of Error in X-Ray Measurements of Residual Stress", J. Appl. Phys. 35, No. 6, 1915 (1964).
5. D. P. Koistinen, and R. E. Marburger, "Calculating Peak Position in X-Ray Residual Stress Measurements of Hardened Steel", Trans. Am. Soc. Metals, 51, 537 (1959).
6. C. J. Kelly and E. Eichen, "Computer Controlled X-Ray Diffraction Measurement of Residual Stress" in L. S. Birks, C. S. Barrett, J. B. Newkirk and C. O. Rudd, Editors, Advances in X-Ray Analysis, 16, 344, Plenum Press (1973).
7. G. Koves and C. Y. Ho, "Computer Automated X-Ray Stress Analysis", Norelco Reporter, 11, 99 (1964).
8. N. W. Tideswell, I. Canner, and H. J. Vanderveldt, "Field X-Ray Diffractometer for Surface Stress Determinations in Naval Structures", Naval Ship Research and Development Center, Report 3568, April 1972.
9. T. E. Davidson, J. E. Throop, A. N. Reiner, "The Role of Fracture Toughness and Residual Stresses in the Fatigue and Fracture Behavior of Large Thick-Walled Pressure Vessels", Watervliet Arsenal Report No. 7184, October 1971.

10. P. J. Cote and G. P. Capsimalis, "Applications of X-Ray Stress Measuring Techniques", Watervliet Arsenal Report No. 7253, October 1972.

WATERVLIET ARSENAL INTERNAL DISTRIBUTION LIST

May 1976

	<u>No. of Copies</u>
COMMANDER	1
DIRECTOR, BENET WEAPONS LABORATORY	1
DIRECTOR, DEVELOPMENT ENGINEERING DIRECTORATE	1
ATTN: RD-AT	1
RD-MR	1
RD-PE	1
RD-RM	1
RD-SE	1
RD-SP	1
DIRECTOR, ENGINEERING SUPPORT DIRECTORATE	1
DIRECTOR, RESEARCH DIRECTORATE	2
ATTN: RR-AM	1
RR-C	1
RR-ME	1
RR-PS	1
TECHNICAL LIBRARY	5
TECHNICAL PUBLICATIONS & EDITING BRANCH	2
DIRECTOR, OPERATIONS DIRECTORATE	1
DIRECTOR, PROCUREMENT DIRECTORATE	1
DIRECTOR, PRODUCT ASSURANCE DIRECTORATE	1
PATENT ADVISORS	1

EXTERNAL DISTRIBUTION LIST

December 1976

1 copy to each

OFC OF THE DIR. OF DEFENSE R&E
ATTN: ASST DIRECTOR MATERIALS
THE PENTAGON
WASHINGTON, D.C. 20315

CDR
US ARMY TANK-AUTMV COMD
ATTN: AMDTA-UL
AMSTA-RKM MAT LAB
WARREN, MICHIGAN 48090

CDR
PICATINNY ARSENAL
ATTN: SARPA-TS-S
SARPA-VP3 (PLASTICS
TECH EVAL CEN)
DOVER, NJ 07801

CDR
FRANKFORD ARSENAL
ATTN: SARFA
PHILADELPHIA, PA 19137

DIRECTOR
US ARMY BALLISTIC RSCH LABS
ATTN: AMXBR-LB
ABERDEEN PROVING GROUND
MARYLAND 21005

CDR
US ARMY RSCH OFC (DURHAM)
BOX CM, DUKE STATION
ATTN: RDRD-IPL
DURHAM, NC 27706

CDR
WEST POINT MIL ACADEMY
ATTN: CHMN, MECH ENGR DEPT
WEST POINT, NY 10996

CDR
HQ, US ARMY AVN SCH
ATTN: OFC OF THE LIBRARIAN
FT RUCKER, ALABAMA 36362

CDR
US ARMY ARMT COMD
ATTN: AMSAR-PPW-IR
AMSAR-RD
AMSAR-RDG
ROCK ISLAND, IL 61201

CDR
US ARMY ARMT COMD
FLD SVC DIV
ARMCOM ARMT SYS OFC
ATTN: AMSAR-ASF
ROCK ISLAND, IL 61201

CDR
US ARMY ELCT COMD
FT MONMOUTH, NJ 07703

CDR
REDSTONE ARSENAL
ATTN: AMSMI-RRS
AMSMI-RSM
ALABAMA 35809

CDR
ROCK ISLAND ARSENAL
ATTN: SARRI-RDD
ROCK ISLAND, IL 61202

CDR
US ARMY FGN SCIENCE & TECH CEN
ATTN: AMXST-SD
220 7TH STREET N.E.
CHARLOTTESVILLE, VA 22901

DIRECTOR
US ARMY PDN EQ. AGENCY
ATTN: AMXPE-MT
ROCK ISLAND, IL 61201

EXTERNAL DISTRIBUTION LIST (Cont)

1 copy to each

CDR
US NAVAL WPNS LAB
CHIEF, MAT SCIENCE DIV
ATTN: MR. D. MALYEVAC
DAHLGREN, VA 22448

DIRECTOR
NAVAL RSCH LAB
ATTN: DIR. MECH DIV
WASHINGTON, D.C. 20375

DIRECTOR
NAVAL RSCH LAB
CODE 26-27 (DOCU LIB.)
WASHINGTON, D.C. 20375

NASA SCIENTIFIC & TECH INFO FAC
PO BOX 8757, ATTN: ACQ BR
BALTIMORE/WASHINGTON INTL AIRPORT
MARYLAND 21240

DEFENSE METALS INFO CEN
BATTELLE INSTITUTE
505 KING AVE
COLUMBUS, OHIO 43201

MANUEL E. PRADO / G. STISSER
LAWRENCE LIVERMORE LAB
PO BOX 808
LIVERMORE, CA 94550

DR. ROBERT QUATTRONE
CHIEF, MAT BR
US ARMY R&S GROUP, EUR
BOX 65, FPO N.Y. 09510

2 copies to each

CDR
US ARMY MOB EQUIP RSCH & DEV COMD
ATTN: TECH DOCU CEN
FT BELVOIR, VA 22060

CDR
US ARMY MAT RSCH AGCY
ATTN: AMXMR - TECH INFO CEN
WATERTOWN, MASS 02172

CDR
WRIGHT-PATTERSON AFB
ATTN: AFML/MXA
OHIO 45433

CDR
REDSTONE ARSENAL
ATTN: DOCU & TECH INFO BR
ALABAMA 35809

12 copies

CDR
DEFENSE DOCU CEN
ATTN: DDC-TCA
CAMERON STATION
ALEXANDRIA, VA 22314

NOTE: PLEASE NOTIFY CDR, WATERVLIET ARSENAL, ATTN: SARWV-RT-TP,
WATERVLIET, N.Y. 12189, IF ANY CHANGE IS REQUIRED TO THE ABOVE.